

# Simulation and Characterization of High Q Microresonators Fabricated by UV – LIGA.

S. Basrour, H. Majjad, J. R. Coudeville, M. de Labachellerie.  
Laboratoire de Physique et Métrologie des Oscillateurs CNRS,  
25044 F Besançon, France. sbasrour@lpmo.edu

## ABSTRACT

This paper is devoted to a study on a new metallic microresonator realized by UV-LIGA technique. This device is excited electrostatically and takes advantage of the contour modes or Lamé-modes of the structure. Design methods of such device are presented and validated by the use of Finite Element Analysis (FEA). Details on the fabrication process are also exposed. The vibration modes are detected with an optical interferometer and preliminary results are presented. A comparison between experiments and numerical predictions are finally discussed.

**Keywords:** MEMS, resonator, Lamé, FEA, UV-LIGA.

## 1 INTRODUCTION

During the last decade, a great number of micro-electro-mechanical resonators have been designed and fabricated using CMOS compatible technologies [1]. Most of these devices, well known as RF MEMS, use out-of-plane or in-plane flexural modes, and are generally fabricated with polysilicon. These devices present low Q's in air and even in vacuum due to different kind of damping [2]. Despite their poor electromechanical properties these transducers have been used for signal processing [3].

The aim of this paper is to propose a new microresonator operating on a contour mode or Lamé-mode. This kind of mechanical mode is expected to exhibit high Q at high frequencies, compared to the Q's reported on flexural resonators.

The first part of this paper presents the electrostatically actuated resonator, which is composed of a plate and two anchors. First, we have estimated the frequency by an analytical model. Using a Finite Element Analysis (FEA), we have taken into account the whole structure and refined our previous simulations.

The second part of this paper is devoted to the technological aspects of the fabrication of the device, and to its characterization. In order to achieve a high aspect ratio, this device is fabricated by UV – LIGA, which is a promising technology for MEMS devices fabricated above IC [4]. The characterization of the device has been performed using a powerful optical bench, which allows the measurements of very weak amplitudes of vibration.

The last section concerns the comparison between the experimental results and the simulations obtained by the FEA.

## 2 DESIGN AND SIMULATIONS

In a basic geometry like a free-standing square plate, the Lamé-mode can be calculated using an analytical model [5]. For that, the plate must be composed by an homogeneous material, with a thickness  $t$  and a side  $L$  with  $L \gg t$ . In this case one can consider the structure as a thin plate submitted to in-plane strain.

In addition, if the material is isotropic, the frequencies associated to the Lamé-mode in a square plate can be given by the following relation:

$$f = \frac{nc}{\sqrt{2} L} \quad (1)$$

where  $n$  is the rank of the mode and  $c$  is the velocity of the vibration and:

$$c = \sqrt{\frac{C_{44}}{\rho}} = \sqrt{\frac{C_{11} - C_{12}}{\rho}} \quad (2)$$

In our case, the elastic components  $C_{44}$  and  $C_{12}$  are equal respectively to the Lamé coefficients  $\mu$  and  $\lambda$ . Thus, we can write :

$$C_{44} = \mu = \frac{E}{2(1+\nu)} \quad \text{and} \quad C_{12} = \lambda = \frac{E\nu}{(1+\nu)(1-2\nu)} \quad (3)$$

$E$  is the Young's modulus of the material and  $\nu$  the Poisson's coefficient. For the electroplated nickel used in the LIGA technique, we have assumed  $E = 195$  GPa  $\nu = 0.34$  and  $\rho = 8960$  kg. m<sup>-3</sup> [6].

One can note that for a given material, the frequency of the structure is tuned only by one geometric parameter i.e. the lateral dimension  $L$ . Moreover, in this elementary structure the nodes of vibration are located at the corners and the center of the plate. From a fabrication point of view, these points can be used as anchors. In figure 1, we report a design of the microresonator composed by a square plate, two anchors and an electrode for the electrostatic excitation of the mode. The parameter  $a$  corresponds to the clamped part of the plate.

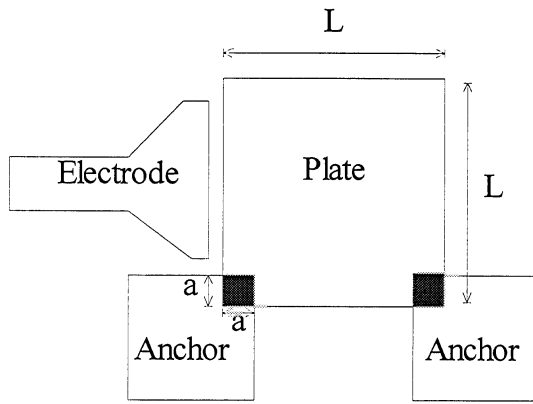


Figure 1: Scheme of the Lamé microresonator.

In this first approach completely idealized, the whole structure is not simulated. Thus, we have performed a FEA with the ANSYS 5.6 Package of the abovementioned device. Figure 2 corresponds to the deformed structure for the first order Lamé-mode ( $n = 1$ ). The sizes of the device are  $L = 336 \mu\text{m}$ ,  $a = 20 \mu\text{m}$  and  $t = 12 \mu\text{m}$ . We have used a SOLID 95 element with 6 DOF for the meshing of the structure. We have even used other elements such as SOLID 92, SOLID 45 for meshing the structure and the effects on the eigenfrequencies are negligible.

The resonant frequencies obtained for the Lamé-mode by the analytical model (free standing plate) and the FEA are :

$$f = \frac{c}{\sqrt{2} L} = 5.99 \text{ MHz and } f_{FEA} = 6.073 \text{ MHz}$$

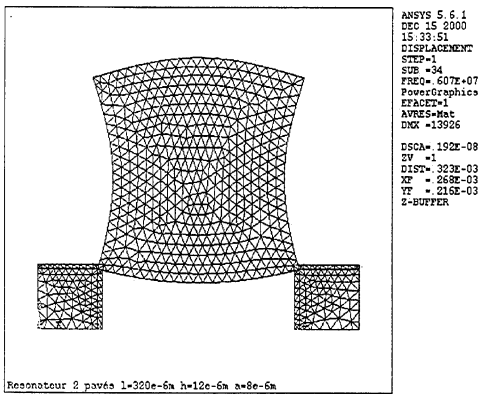


Figure 2: Finite Element simulation of the Lamé-mode.

The analytical model gives, with a good approximation, the resonant frequency of the device and can be used in the preliminary steps of the design of the resonator. The FEA provides more details, in particular on the appearance of parasitic modes due to the out-of-plane vibrations of the plate. The frequencies of these undesirable modes are located before and after the Lamé-mode and then can be responsible of the decrease in the coupling between the electrical energy provided by the electrical port and the mechanical resonator.

For instance, we report in figure 3 the influence of the thickness  $t$  of the device on the Lamé-mode frequency and its rank.

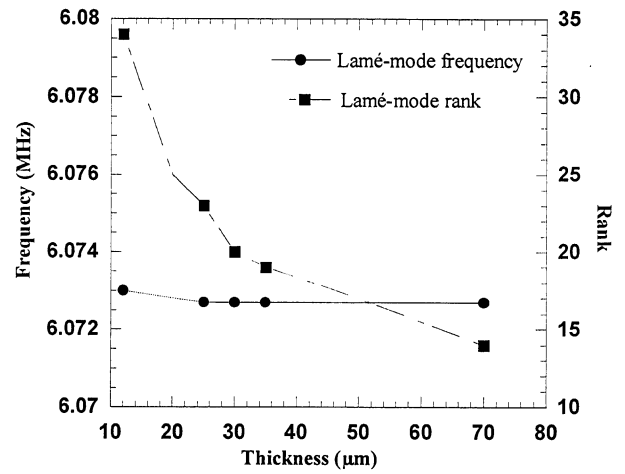


Figure 3: Effect of the thickness  $t$  on the Lamé frequency.

One can note that the Lamé-mode frequency is insensitive to this geometrical parameter but the rank of the mode decreases drastically when  $t$  exceeds  $20 \mu\text{m}$ .

In figure 4, we report the effect of the parameter  $a$  associated to the anchor on the frequency of the Lamé-mode as well as the two nearest frequencies associated to the parasitic modes.

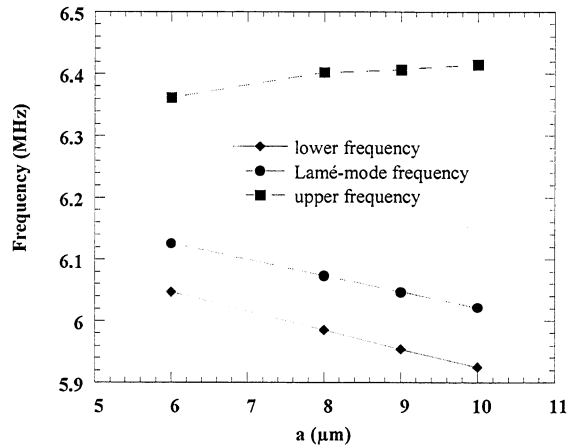


Figure 4: Effect of the parameter  $a$  on the Lamé frequency ( $t = 25 \mu\text{m}$ ).

This parameter affects the Lamé-mode frequency and the lower frequency in the same way and the shift is in tens kHz. Furthermore  $a$  increases the higher frequencies. From the mechanical point of view, the devices with high aspect ratios ( $t/a$ ) present a better decoupling between the Lamé-mode and the adjacent frequencies. We noticed that the parameter  $a$  must be the smallest for diminishing the losses via the anchors. Moreover, high aspect ratios devices lead to high capacitance and then a better coupling between the electrical and mechanical energies. With these results in mind the final sizes of the device are  $a = 8 \mu\text{m}$ ,  $L = 336 \mu\text{m}$ , and  $t = 12 \mu\text{m}$ .

### 3 FABRICATION PROCESS

High aspect ratio devices can be achieved by different techniques such as X Ray LIGA [7] or deep RIE [8]. UV – LIGA presents lower aspect ratios but recent papers show that this method can be used for the fabrication of MEMS above IC [9].

We report in figure 5 the flow chart of the process used for the fabrication of the microresonator. First, the silicon substrate is oxidized ( $1.2 \mu\text{m SiO}_2$ ). Then the sacrificial layer is patterned ( $2 \mu\text{m Al}$ ). The Gold seed layer is sputtered and enables the electroplating of the nickel. The molds have been performed with a  $20 \mu\text{m}$  thick SJR 5740 (Shipley) photoresist. The nickel was electroplated using a commercial bath of nickel sulfamate optimized for a low stress deposition ( $T = 55 \text{ }^\circ\text{C}$ ,  $\text{pH} = 4$ ,  $J = 10 \text{ mA.cm}^{-2}$ ).

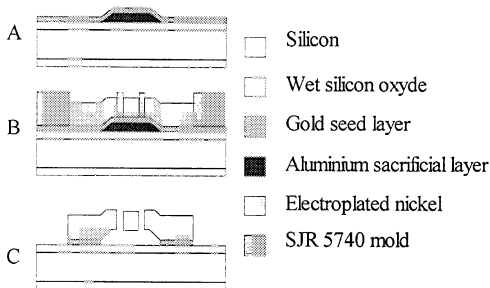


Figure 5: Flow chart for the UV- LIGA process.

A close up view of the device is reported in the SEM photos of figure 6. In this case the thickness  $t$  of the electroplated structure is  $12 \mu\text{m}$ .

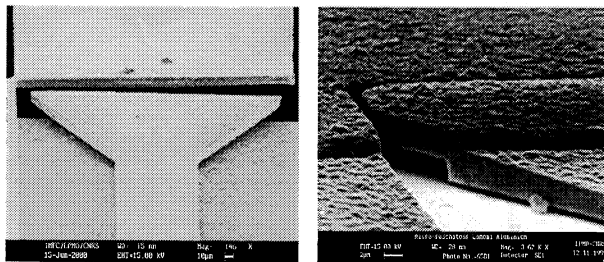


Figure 6: Close up views of the Lamé resonator.

### 4 EXPERIMENTAL CHARACTERIZATION

At the moment, the Lamé-mode and the parasitic modes have been detected by the aim of an optical interferometer described in figure 7 [10]. This system allows the measurement of weak amplitudes of vibration down to  $5 \cdot 10^{-12} \text{ m}$  and the micropositioning table (XY) enables the acquisition of an image corresponding to an out-of plane vibration mode. The device was excited by superposing an DC voltage (not represented) and the AC voltage given by the Network analyzer. The amplitude of this AC voltage is amplified by a wideband amplifier in order to achieve an amplitude of  $8 \text{ V}$  up to  $20 \text{ MHz}$ .

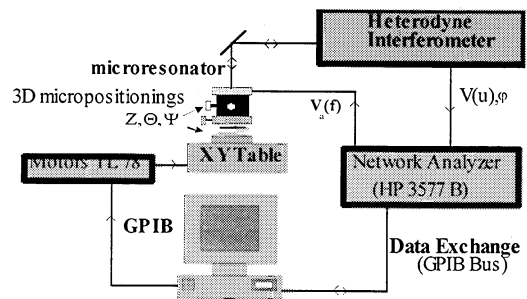


Figure 7: Optical bench for the characterization of vibration modes.

### 5 RESULTS AND DISCUSSIONS

The Lamé-mode has been recorded with the Laser beam focused on the opposite side according to the side facing the electrode (figure 8). The frequency observed is  $6,051 \text{ MHz}$  and the  $Q$  at  $-3 \text{ dB}$  is  $1210$  which is much better than most of the values measured up-to-date in air [3]. This quality factor is obtained because the resonator is attached at its nodal points (i.e. the corners). In this configuration the energy dissipated in the support via the anchors is minimized.

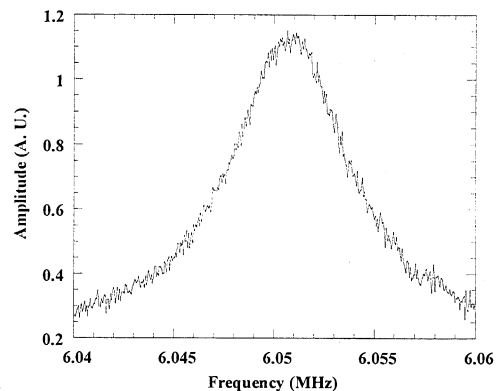


Figure 8: Optical detection of the Lamé mode ( $f = 6.051 \text{ MHz}$ ,  $Q = 1210$ ,  $AC = 8.2 \text{ V}$ ,  $DC = 63 \text{ V}$ ).

We have also identified parasitic modes linked to the out-of-plane bending modes. In figure 9a, we give an example of the amplitude of the vibration obtained for the fourth mode.

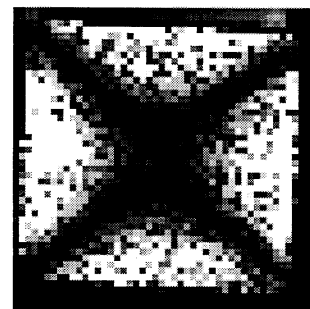


Figure 9: Amplitude's image for the 4th mode at  $604 \text{ kHz}$ ,  $AC = 2.5 \text{ V}$ ,  $DC = 63 \text{ V}$ .

The SEM observations of the device show a trapezoidal cross section of the plate due to the losses in resolution during the lithography. Taking into account the exact geometry of the plate (figure 10) in our finite element model we have obtained a good agreement between simulations and the experimental data for the Lamé-mode and also for the out-of-plane parasitic modes.

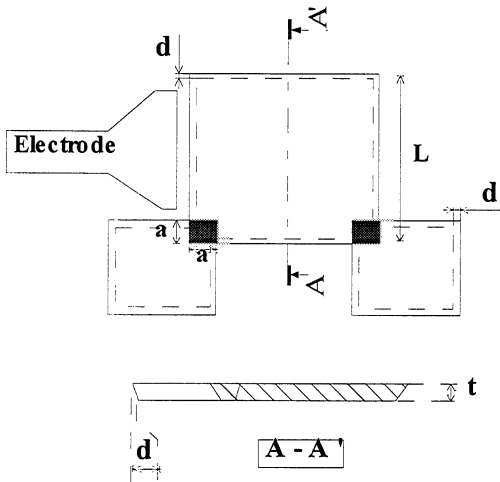


Figure 10: Scheme of the trapezoidal section used in the finite element model.

The difference between the simulations and the experimental results is less than 5 kHz for these two modes. The figure 11 represents the simulated fourth mode of the plate (606 kHz) which can be compared to the real image of this mode (figure 9).

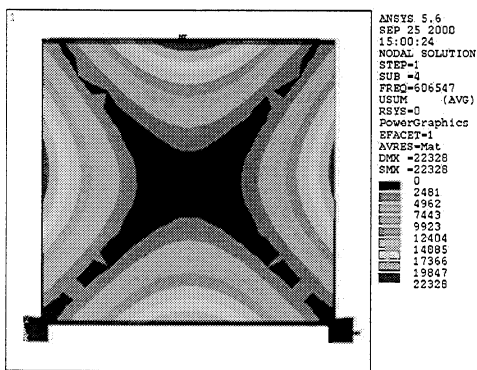


Figure 11: FEM simulation of the 4th mode with real geometric values ( $f = 606$  kHz).

The figure 12 gives the frequency of the simulated Lamé-mode with the real geometry of the plate (6.05 MHz).

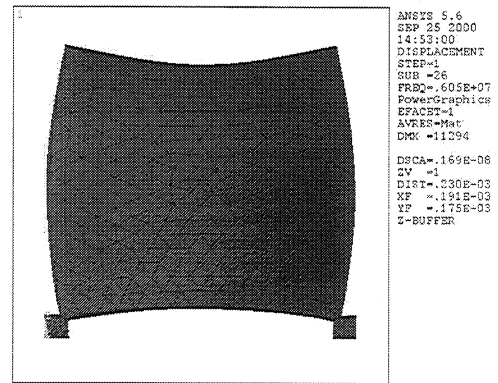


Figure 12: FEM simulation of the Lamé-mode with real geometric values ( $f = 6.05$  MHz).

## 6 CONCLUSION

Previous works have showed the interest of the Lamé resonator to make temperature sensors [11]. In this paper, we have presented first results on a new Lamé-microresonator. We have found a good agreement between finite element simulations and the experimental results for the Lamé-mode and also for the out-of-plane parasitic modes. Then the FEA seems to be a powerful method for CAD of these microresonators.

New structures are under test for the electrical characterization in vacuum.

## REFERENCES

- [1] K. Wang, C. T.-C. Nguyen, Proc. of the IEEE International Micro Electro Mechanical Systems Workshop, Nagoya, Japan, 1997.
- [2] H. Hosaka, K. Itao, S. Kuroda, Sensors and Actuators, A49, 102-107, 1995.
- [3] L. Lin, R. T. Howe, P. Pisano, J of MEMS, Vol 7, N° 3, 286-294, 1998.
- [4] M. Wycisk, T. Tönnesen, J. Binder, S. Michaelis, H. - J. Timme, Sensors and Actuators, A83, 93-100, 2000.
- [5] C. Bourgeois, Proc. 34th ann. Freq. Control. Symposium, 1980.
- [6] H. Majjad, S. Basrou, P. Delobelle, M. Schmidt, Sensors and Actuators, A74, 148-151, 1999.
- [7] R.K. Kupka, F. Bouamrane, C. Cremers, S. Megter, Applied Surface Science, 164, 97-110, 2000.
- [8] F. Ayela, J. L. Bret, J. Chaussy, T. Fournier, E. Menegaz, Rev. of Sci. Instrum., vol. 71, 5, 2211-2217, 2000.
- [9] H. Lorenz, M. Dupont, N. Fahrni, J. Brugger, P. Vettiger, P. Renaud, Sensors and Actuators, A64, 33-39, 1998.
- [10] B. Cretin, W.-X. Xie, S. Wang and D. Hauden, Opt. Com., 65, 157-162, 1988.
- [11] H. Kanie, H. Kawashima, IEEE Transactions on U. F. F. C., Vol. 47, No. 2, 341-345, 2000.